PHYSD2598

ELSEVIER

Physica D 2598 (2000) 1–12

PHYSICA D

www.elsevier.com/locate/physd

Nonlinear response of the sine-Gordon breather to an a.c. driver

K. Forinash [a,*], C.R. Willis [b]

[a] *Division of Natural Sciences, Indiana University Southeast, 4201 Grant Line Road, New Albany, IN 47150-6405, USA*
[b] *Department of Physics, Boston University, 590 Commonwealth Avenue, Boston, MA 02215, USA*

Received 10 January 2000; received in revised form 28 September 2000; accepted 29 September 2000
Communicated by I. Gabitov

Abstract

We investigate the nonlinear response of the continuum sine-Gordon (SG) breather to an a.c. driver. We use an ansatz by Matsuda which is an exact collective variable (CV) solution for the unperturbed SG breather and uses only a single CV, $r(t)$, which is the separation between the center of masses of the kink and antikink that make up the breather. We show that in the presence of a driver with an amplitude below the breakup threshold of the breather into kink and antikink, the a.c.-driven SG is quite accurately described by the $r(t)$, which is a solution of an ordinary differential equation for a one-dimensional point particle in a potential $V(r)$ driven by an a.c. driver and with an r-dependent mass, $M(r)$. That is below the threshold for breakup, the solution for a driven $r(t)$ and the use of the Matsuda identity gives a solution for the a.c.-driven SG, which is very close to the exact simulation of the a.c.-driven SG. We use a wavelet transform to analyze the frequency dependence of the time-dependent nonlinear response of the SG breather to the a.c. driver. We find the wavelet transforms of the CV solution and of the simulation of the a.c.-driven SG are qualitatively very similar to each other and often agree quite well quantitatively. In cases of breakup of the breather into K and A, where there is no appreciable radiation of phonons, we find the CV solution is very close to the exact simulation result.

PACS: 05.40.+j; 03.40.-t; 74.50.+r

Keywords: Sine-Gordon; Collective variable solution; Kink-antikink interactions

1. Introduction

In this paper, we use a collective variable (CV) approach to investigate the nonlinear response of a continuum sine-Gordon (SG) breather to an a.c. driver which satisfies the differential equation

$$\phi_{,tt} - \phi_{,xx} + V_{,\phi} = 0,$$
$$V(\phi) \equiv \Gamma_0^2(1 - \cos\phi)\varepsilon f(t)\phi \qquad (1.1)$$

where $f(t)$ is the a.c. driver, ε the strength of the driver and Γ_0^2 dimensionless. The CV, $r(t)$, is the separation between the center of mass of the kink (K) and the antikink (A) that make up the breather. The equation of motion for the one-dimesional "particle" $r(t)$ is given by Newton's law for a particle whose mass, $M(r)$, depends on r moving in a potential $U(r)$ derived in [1] and driven by an a.c. driver, see Eq. (2.4). In the absence of the a.c. driver the solution, $r(t)$, when inserted into the Matsuda identity [2] gives the rigorous solution of the SG breather. When we add the a.c. driver to the $r(t)$ equation of motion, solve for $r(t)$,

* Corresponding author.
E-mail address: kforinas@ius.edu (K. Forinash).

0167-2789/00/$ – see front matter
PII: S0167-2789(00)00194-9

and substitute into the Matsuda identity we obtain an approximate solution for the SG breather in the presence of the a.c. driver. The solution in the presence of the driver is only approximate because the identity is only exact for the undriven breather. However, as we show in Section 3, the approximate CV solution for the breather is very close to the exact simulation result for the a.c.-driven SG for driver amplitudes below the amplitude for the breakup of the breather into K and A. In some cases even at breakup of the breather into K and A the CV solution is very close to the exact simulation result. Consequently we are able to obtain quite-detailed knowledge of the nonlinear response of the SG solution to an a.c. driver by analyzing the solution of a one-dimensional ordinary differential equation for $r(t)$ which yields the exact breather solution when the a.c. driver is not present.

The frequencies that appear in $r(t)$ due to the nonlinear particle potential, $U(r)$, agree very well qualitatively and quantitatively with the simulation of the full a.c.-driven SG equation. Also the amplitude of the driver required for the breakup of the breather into K and A agree qualitatively and fairly well quantitatively. For the range of driver amplitudes and frequencies used in this paper we find the intensity of the phonons radiated to be small even in the case of breakup of the breather into K–A. The main reason that phonon radiation is small is that $r(t)$ has to be driven nonlinearly away from its (nonlinear) motion in the undriven case before there can be radiation of phonons. Below the threshold for breakup the radiation intensity, $I = \varepsilon^{2m}$, where $m > 1$ and ε is the dimensionless driver amplitude which we take in this paper to be in the range $0.04 \leq \varepsilon \leq 0.2$. Near breakup only a linear deviation from the undriven $r(t)$ is needed to cause the radiation of the phonons observed in the simulations.

We compare the frequency spectrum of the CV approximation with the exact simulation of the driven SG by using a wavelet description which enables us to see the frequencies that appear in both the CV approximation and the simulation of the full a.c.-driven continuum SG equation at different times in their evolution. For example we find that below the threshold for breakup both the CV approximation and the exact simulation show a nonlinear frequency "beating" between the driver and the breather which shows up in the phonon band. We also find that in all cases when the exact simulation undergoes breakup into a K and A the CV approximation also breaks up into a K and A.

The nonlinear response of the undamped a.c.-driven SG breather in this paper is time dependent and contains a spectrum of frequencies with variable amplitudes which depend sensitively on the amplitude and frequency of the driver. The nonlinear response contrasts with the damped a.c.-driven SG [3] where the main response is a constant shift (modulation) of the undriven breather frequency which depends on the driver amplitudes, driver frequency and on the fixed value of the energy of the kink. The fixed energy is determined by balancing the energy loss due to damping with the energy gain from the driver. In Section 2, we derive the equations of motion for $r(t)$.We compare the results for the CV approximation with the simulation of the a.c.-driven SG in Section 3. In Section 4, we summarize and conclude the paper.

2. CV equations of motion

We first briefly review the results for the rigorous single CV theory of the breather and the K–A system. The analytic solution for the breather is

$$\phi_{\mathrm{b}}(x,t) = 4\tan^{-1}\left[\frac{\Gamma_{\mathrm{b}}\cos(\omega t-\theta)}{\omega_{\mathrm{b}}\cosh(\Gamma x)}\right], \tag{2.1}$$

where the center of mass of the breather is located at zero, θ determines the initial phase, ω_{b} is the breather frequency and $\Gamma_{\mathrm{b}} < 1$ obeys the dispersion law $\omega_{\mathrm{b}}^2 + \Gamma_{\mathrm{b}}^2 = 1$. From Matsuda's identity for the breather [2], we define $r(t)$ by

$$r(t) \equiv \frac{2}{\Gamma_{\mathrm{b}}}\sinh^{-1}\left[\frac{\Gamma_{\mathrm{b}}}{\omega_{\mathrm{b}}}\cos(\omega t-\theta)\right]. \tag{2.2}$$

When we substitute Eq. (2.2) in the analytic solution, (2.1), and use the following identity $\tan^{-1} y - \tan^{-1} z = \tan^{-1}[y - z/(1+yz)]$, we obtain

$$\phi(x,t) = 4\tan^{-1}\mathrm{e}^{\Gamma(x-r(t)/2)} - 4\tan^{-1}\mathrm{e}^{\Gamma(x+r(t)/2)}, \tag{2.3}$$

where here and in the remainder of the paper we drop the subscript b on Γ, ϕ and ω. Eq. (2.3) is also the exact solution for K–A when we replace Γ by $\gamma \equiv (1 - \frac{1}{4}\dot{r}^2)^{-1/2}$ and $r(t)$ is given by

$$r(t) = 2\gamma^{-1} \sinh^{-1}\left[\frac{2}{\dot{r}} \sinh \frac{\gamma \dot{r} t}{2}\right].$$

For details, see [1]. The close relationship between the exact breather and the K–A solution follows from the fact that the breather is a bound state and the K–A is an unbound state of the "same" potential $U(\Gamma, r)$, where $\Gamma > 1$ for K–A and $\Gamma < 1$ for the breather.

The Hamiltonian for the rigorous single CV equations of motion for the $r(t)$ for the breather and K–A derived in [1] is

$$H = \frac{P_\mathrm{r}^2}{4M_\mathrm{r}} + U(r) + 8(\Gamma + \Gamma^{-1}) + V_\mathrm{ext}(r)$$

with

$$\dot{r} = \frac{P_\mathrm{r}}{2M_\mathrm{r}}, \qquad \dot{P}_\mathrm{r} = \frac{P_\mathrm{r}^2}{4M_\mathrm{r}} \frac{\mathrm{d} \ln M_\mathrm{r}}{\mathrm{d}r} - \frac{\mathrm{d}U}{\mathrm{d}r} - \frac{\mathrm{d}V_\mathrm{ext}}{\mathrm{d}r},$$

where

$$M_\mathrm{r}(r) \equiv 2\Gamma[1 + \Gamma r \,\mathrm{csch}(\Gamma r)]. \tag{2.4}$$

The potential is

$$U(r) \equiv \frac{16\Gamma^{-1}}{\sinh(\Gamma r)} \left\{-\frac{1}{2}\Gamma^3 r - \frac{1}{2}\Gamma r + \Gamma r \coth^2(\Gamma r) - \coth(\Gamma r) - \left(\frac{\Gamma r \coth(\Gamma r) - 1}{\sinh(\Gamma r)}\right)\right\}.$$

When the solution of Eq. (2.4) with $V_\mathrm{ext} = 0$, for r with $\Gamma < 1$ is substituted in Eq. (2.1) we get the exact SG breather solution. When the solution of Eq. (2.4) for r with $\Gamma = \gamma > 1$ is substituted in Eq. (2.1) we get the exact K–A solution. Next we add the a.c. driver whose potential is $V_\mathrm{ext}(r) \equiv 4\varepsilon f(t) \int_{-\infty}^{\infty} \mathrm{d}x \{\tan^{-1} \Gamma(x - \frac{1}{2}r) - \tan^{-1} \Gamma(x + \frac{1}{2}r)\}$, where $f(t) = \varepsilon \sin \Omega t$.

Note that $\mathrm{d}V_\mathrm{ext}/\mathrm{d}r = -16\varepsilon\Gamma f(t)$ and $\mathrm{d}V_\mathrm{ext}/\mathrm{d}\Gamma = 0$. Thus the a.c. driver drives $r(t)$ directly. However, even if Γ was treated as a dynamical variable the a.c. driver would not drive Γ directly, i.e., $\Gamma(t)$ would experience the driver only through the driver's effect on $r(t)$.

3. Comparison of CV approximation with simulation

In this section, we analyze some typical cases of the a.c.-driven SG for the full SG partial differential equation (S) and for the CV description determined by the solution $r(t)$ of the ordinary differential equation (2.4) substituted in Eq. (2.3). Our purpose is to first examine the time-dependent nonlinear response of the SG breather to the a.c. driver and second to show how the much simpler CV description which is completely determined by the solution $r(t)$ of Eq. (2.4), provides us with information that appreciably increases our understanding of the nonlinear response of the SG breather to an a.c. driver. In order to compare the CV calculation with the full simulation equations (S) of the SG breather they were both iterated with a standard fifth-order Runge–Kutta method [4] and their output compared. Typically in the absence of a driver with a time step of 0.01 the energy is conserved to an accuracy of 0.001% over a whole simulation which lasted on the order of 300 time units. With a driver the energy is not expected to be conserved exactly, however, in all cases the energy fluctuated around a constant average energy which did not increase or decrease significantly over the length of the simulations. Different initial phase conditions were examined and found to affect mainly the time needed until breakup (driving in resonance was extremely sensitive). To avoid questions related to phase the driver was turned on very slowly (over 10–20 time units) in most cases except where noted.

We find that a very useful technique to present frequency and time-dependent information in our simulations is to use a wavelet transform [5]. The underlying idea of the wavelet transform used in this paper is similar to that of the "windowed" Fourier transform defined by

$$Tf(t, \xi) = \int_{-\infty}^{\infty} f(x) g(x - t)\, \mathrm{e}^{-\mathrm{i}2\pi\xi x}\, \mathrm{d}x \tag{3.1}$$

which is the Fourier transform with a window function g inserted, which limits the calculation of frequency to an interval of time around time t. (The window function g can be chosen to be a Gaussian, which results in

a Gabor transform.) The wavelet transform we use differs from this transform in that the "window" changes width as the frequency ξ is changed. For high frequencies, the window is narrow (which will catch rapid changes in frequency better); for low frequencies, the window is wider (which localizes frequency better). The continuous wavelet transform is well suited for localizing frequency and for localizing time whereas the windowed Fourier transform can often localize one domain well but not the other.

An inherent limitation of the transform restricts how well time and frequency can simultaneously be localized with this method. In a fashion mathematically similar to the uncertainty principle, both time and frequency domains cannot be made arbitrarily small. This limitation manifests itself in our graphs as a trade-off between how "blurry" the image is vertically (i.e., localization of frequency), and how blurry the image is horizontally (i.e., localization of time).

Wavelet transforms were performed on the amplitude oscillations of the central site of the breather as the breather evolved in time. The continuous wavelet transform of Grossman and Morlet was used which, for a function f on the line, is defined by

$$Wf(t,\xi) = \int_{-\infty}^{\infty} f(x)\omega(\xi(x-t))\xi \,\mathrm{d}x,$$
$$\omega(x) = \left(\frac{1}{\sigma\sqrt{2\pi}}\right) \mathrm{e}^{\mathrm{i}2\pi x}\, \mathrm{e}^{-x^2/2\sigma^2}. \tag{3.2}$$

The transform $Wf(t,\xi)$ shows information about the strength of the signal f at time t and frequency ξ. Intensity plots (often called spectrograms) of frequency versus time are rendered as graphs showing the intensity of the frequencies present as a function of time. The graphs are arbitrarily scaled to fit the range of intensity values.

We start with a comparison of the full SG, Eq. (1.1), with the CV approximation using the solution of Eq. (2.4) for $r(t)$ for some typical values of the parameters. Although we examined a wide range of breather and driver frequencies in this paper we present only the $\omega = 0.9$ and 0.7 results because as the breather frequency is decreased the discreteness of the simulations starts to become important and the radiation of phonons due to the Peirels–Nabarro potential then interfere with the radiation of phonons caused by the nonlinearity in $r(t)$ produced by the driver.

In Fig. 1 we compare the shape of the SG breather in the simulation of the a.c.-driven SG breather (solid line) and for the CV approximation of the a.c.-driven SG (dotted line). Note that the CV approximation agrees with S in the diagram very closely everywhere but in the wings of the line. We found this agreement is maintained for long periods of time in all cases below threshold for breakup. In Fig. 1 the total number of breather oscillations at this point has been 42 oscillations for the simulation and 43 oscillations for the CV calculation. The reason for the oscillation in the wings of the simulation S but not in the CV is because the CV approximation does not possess phonon degrees of freedom but the simulation S does. The oscillation has a frequency of approximately 1.08 (where the phonon band edge has a frequency of 1 in our units) which is very close to the SG breather quasimode (see [6]). The quasimode is caused by the oscillation of the shape of a kink or a breather and since the frequency is in the phonon band near the band edge it is a quasimode and not a pure mode. The corresponding mode in the ϕ^4 equation is in the gap and is a pure mode. We find that the quasimode is produced at $t = 0$ in S because when the a.c. driver is applied at $t = 0$ it causes an instantaneous change in the shape of the breather which then oscillates and radiates phonons of frequency of 1.08. Thus we find that CV and S are remarkably close together and differ at long times because of the quasimode radiation of phonons. If the a.c. driver is turned on sufficiently slowly the quasimode will not be excited and S and CV will remain close to each other as long as the a.c. driver is well below the threshold for breakup. In some cases (see Fig. 3a and b) we find S radiates phonons due to the interaction of the a.c. driver with the nonlinear breather oscillations which are not related to slope oscillations. Near breakup of the breather into K and A for appreciable driver amplitudes there can be instability, chaotic behavior and sometimes copious radiation of phonons which for the full simulation may lead to a breakup into multiple breathers rather than K–A. In most of the cases we investigated at breakup the phonon radiation is weak and there is a strong similarity between

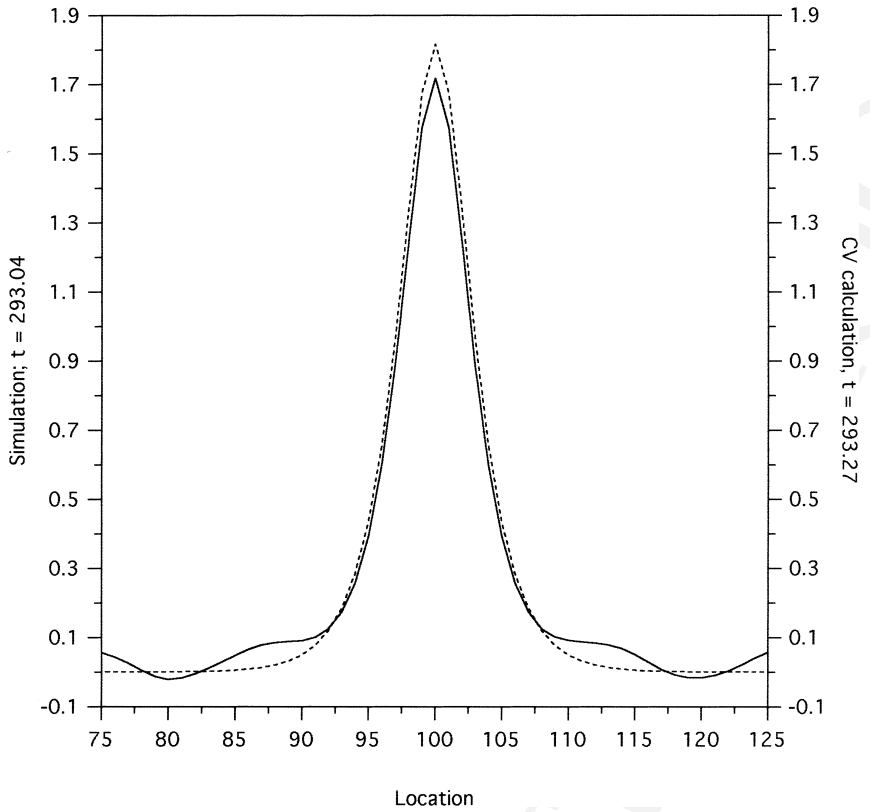

Fig. 1. Simulation and CV calculation of the breather shape captured at maximum amplitude shortly before 300 time units. The breather frequency is 0.9, the driver frequency is 0.7 and the driver amplitude is 0.02 in dimensionless units.

S and CV breakdown when the a.c. driver has a small amplitude.

The amplitude of the driver required for breakup into K and A as a function of the driver frequency is presented in Fig. 2. Except at very low driving frequency $\Omega = 0.1$ and resonance $\Omega = 0.9$ the threshold amplitude for breakup for S and CV are close to each other. When the driving frequency is resonant with the breather frequency the agreement with S and CV breaks down because at resonance a large number of phonons are radiated. It is somewhat surprising that the agreement between S and CV at breakup away from the resonance is so good. Different initial phases were tried and found only to affect the length of time until breakup. Fig. 2 is for in-phase initial conditions.

In Fig. 3a and b we show the breakup of the breather into K–A for S and for CV for $\Omega = 0.4$, $\omega = 0.7$ and driving amplitude of 0.1. In the time before breakup S and CV agree very well and the times of breakup differ by only seven time steps. After breakup K and A recede from each other at the same speed and K and A each oscillate at the driving frequency. However, it is clear that there is a difference in the speed of the K (and A) in S which is 0.17 and the speed of the K (and A) in CV which is 0.70. The reason for the difference speeds in S and CV is that at breakup S radiates phonons while the CV solution cannot radiate phonons. The total energy is approximately the same in both cases and the total rest energy is the same in both cases. Thus the energy radiated by phonons in S shows up as higher kinetic of K and A in the CV calculation. An examination of the amplitude at smaller scales shows phonons present in the simulation case. Most breakups were into K–A pairs but oc-

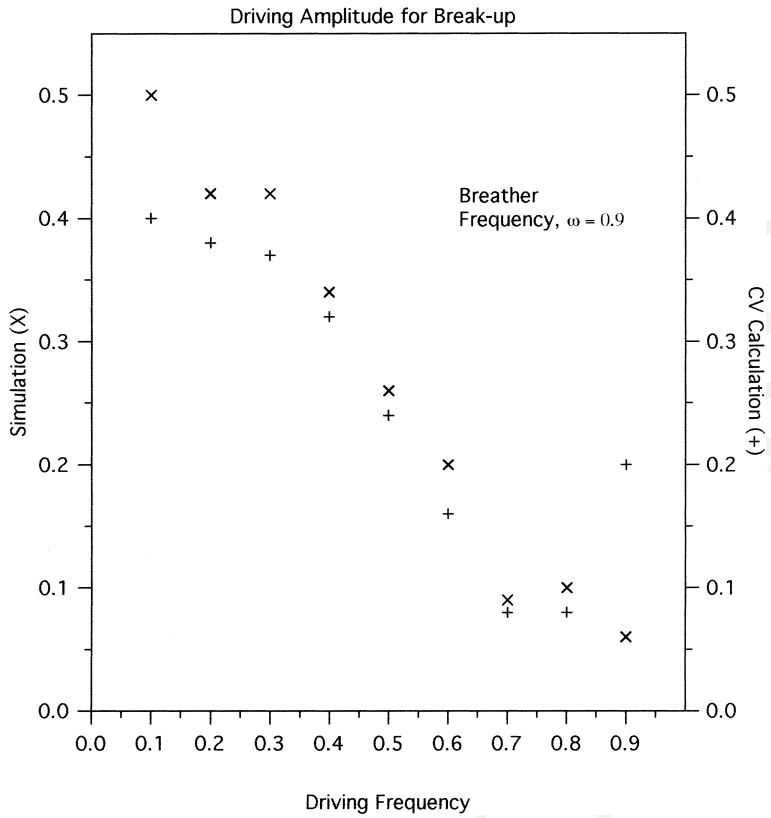

Fig. 2. Driving amplitude needed to cause breakup within 300 time units with various driver frequencies for a breather with a frequency of 0.9, driver on from the beginning. Simulation values are denoted by $\times$, CV calculation by $+$.

casionally the simulation broke up into two smaller breathers.

In Fig. 4a and b we show the wavelet transform of a breather with $\omega = 0.9$, $\Omega = 0.6$ and amplitude $= 0.1$ which is well below breakup. The driver is turned on gradually over 10 time units starting at $t = 50$. We see that there are frequencies above the band edge around 1.15 in both S and CV. These frequencies arise from the nonlinear breather oscillation driven by the a.c. driver. In the simulation these frequencies lead to radiation of phonons. A beating between ω and Ω can be seen in both case with a time duration of about 10 time units. (The small variations in intensity of approximately five time units are an artifact of the calculation and are not physical.) There is a faint intermediate frequency between and just below the frequency 0.8 in both S and CV. Also there is a faint frequency at the band edge in both S and CV. The CV calculation shows the breather frequency shifts downward slightly while the simulation does not because the simulation is radiating phonons which causes the frequency to rise thus canceling the drops in frequency.

In Fig. 5a and b we show the wavelet transform with $\omega = 0.9$, $\Omega = 0.8$ and amplitude $= 0.1$ which is just above breakup for S and just below breakup for CV with the driver turned on gradually over 10 time units starting at $t = 50$. The frequency shifts down to the driver frequency in both S and CV. At $t = 150$ the breakup of S into K and A is complete. In the time between $t = 50$ and 150 the agreement between S and CV for frequencies at 0.9 and below is very good with bands around 0.8, between 0.6 and 0.7 and be-

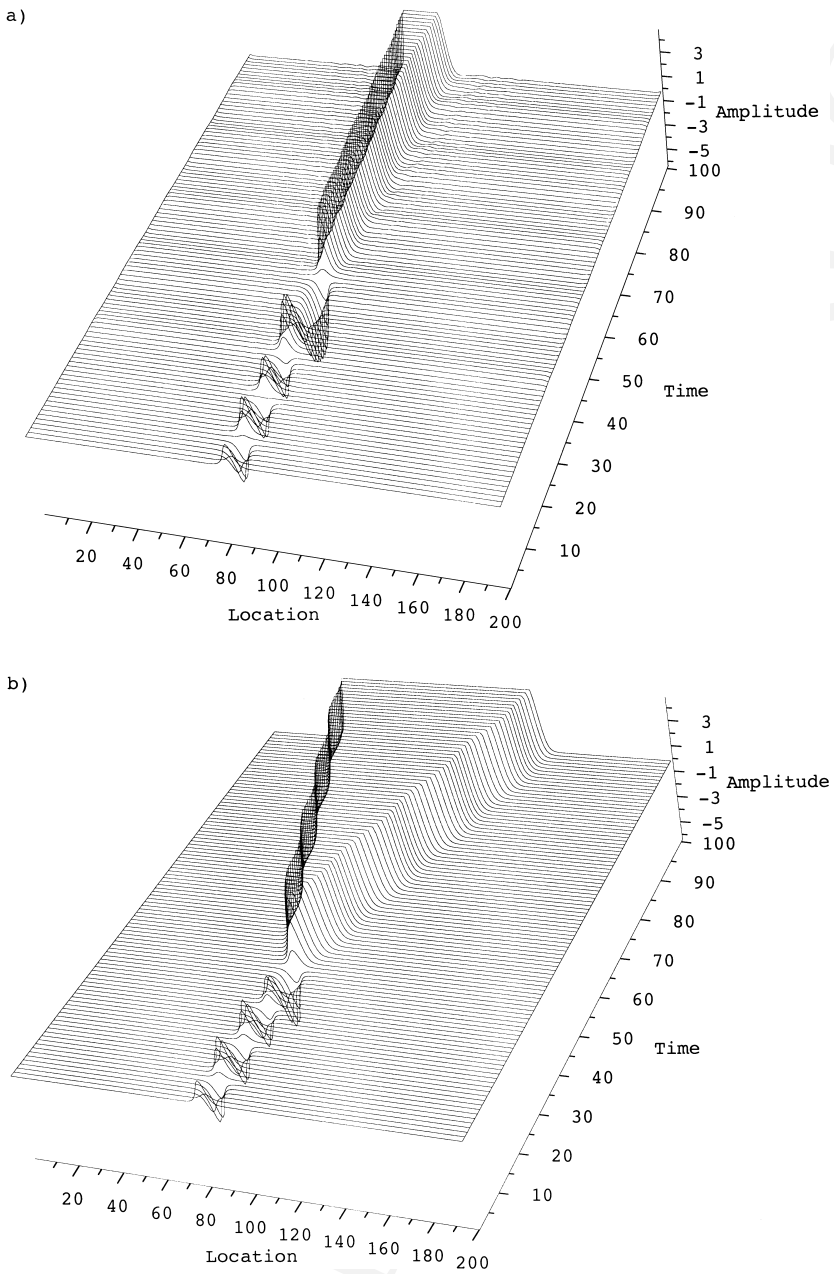

Fig. 3. Breather breakup into kink–antikink pair (simulation (a), CV calculation (b)). Driving frequency is 0.4, breather frequency is 0.7 and driving amplitude is 0.1. Speed of the kink (or antikink) after breakup is approximately 0.17 for the simulation and 0.70 for the CV calculation.

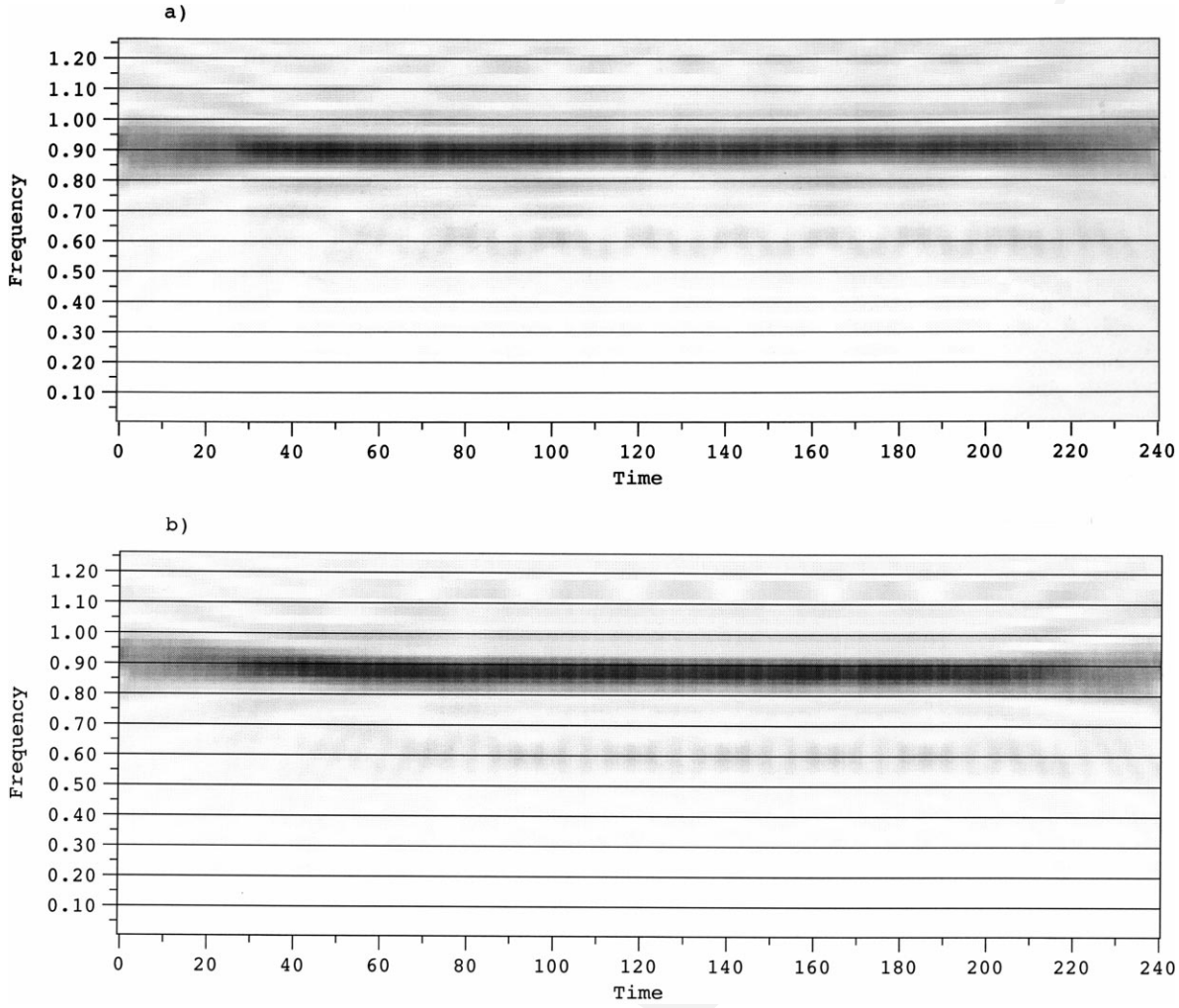

Fig. 4. Wavelet transform of the central location of the breather with initial frequency 0.9, driver frequency 0.6 and amplitude 0.1 (well below breakup). The wavelet transform of the simulation is shown in (a), the CV calculation in (b). The small variations in intensity of approximately five time units are an artifact of the calculation and are not physical.

tween 0.4 and 0.5. Since the CV solution cannot radiate or have shape mode oscillations we can reasonably conclude that the frequencies in the phonon band in the CV solution arise from the interaction between the driver frequency and the frequencies which arise from the difference between the undriven and driven $r(t)$. The frequency spectra of the simulation and the CV calculation are nearly identical (as was the case for all wavelet transforms for cases below breakup).

As a final example of the use of the CV, $r(t)$, to increase our understanding of the a.c.-driven SG we consider the cases with the same driving frequency $\Omega = 0.7$, breather frequency $\omega = 0.9$ and three different but close driving amplitudes of 0.119765, 0.119768 and 0.119770 shown in Fig. 6. In all three cases the SG breather breaks up into K and A. In most cases we examined the breakup occurs smoothly as in Fig. 6a. In Fig. 6b (which differs by only a rela-

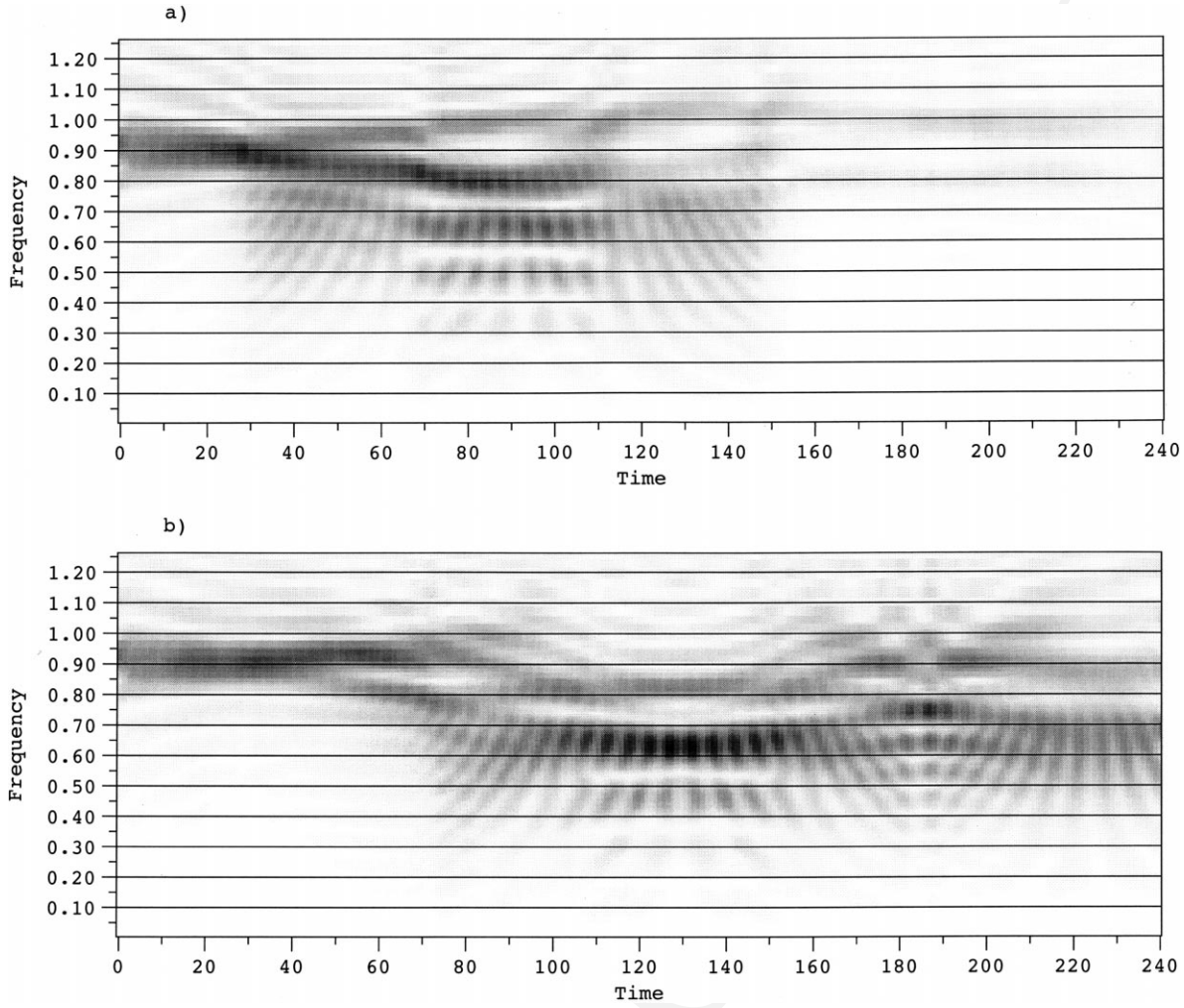

Fig. 5. Wavelet transform of the central location of the breather with initial frequency 0.9, driver frequency 0.8 and amplitude 0.1 (right at breakup for simulation (a), just below breakup for CV calculation (b)). The small variations in intensity of approximately five time units are an artifact of the calculation and are not physical.

tive percentage of the driver amplitude from Fig. 6a of 0.0025%), we see irregular behavior for an appreciable time before breakup. In Fig. 6c (which differs only by a relative percentage change of the driver amplitude from Fig. 6b of 0.0017%), we see the development of a multifrequency quasiperiodic modulation of the breather frequency which might be signaling the onset of chaotic behavior. The three very different results for three nearly equal driver amplitudes demonstrate very effectively the efficacy of using the CV, $r(t)$, to understand the a.c.-driven SG in the breakup region.

The cases we discussed in this section are typical and are a representative selection from the many cases we simulated. In the region away from breakup the agreement is very good. The only significant qualitative difference is that for S phonons can be radiated which only has an appreciable effect for cases near breakup. For cases of breakup where phonon radiation is low there is good agreement between S and CV.

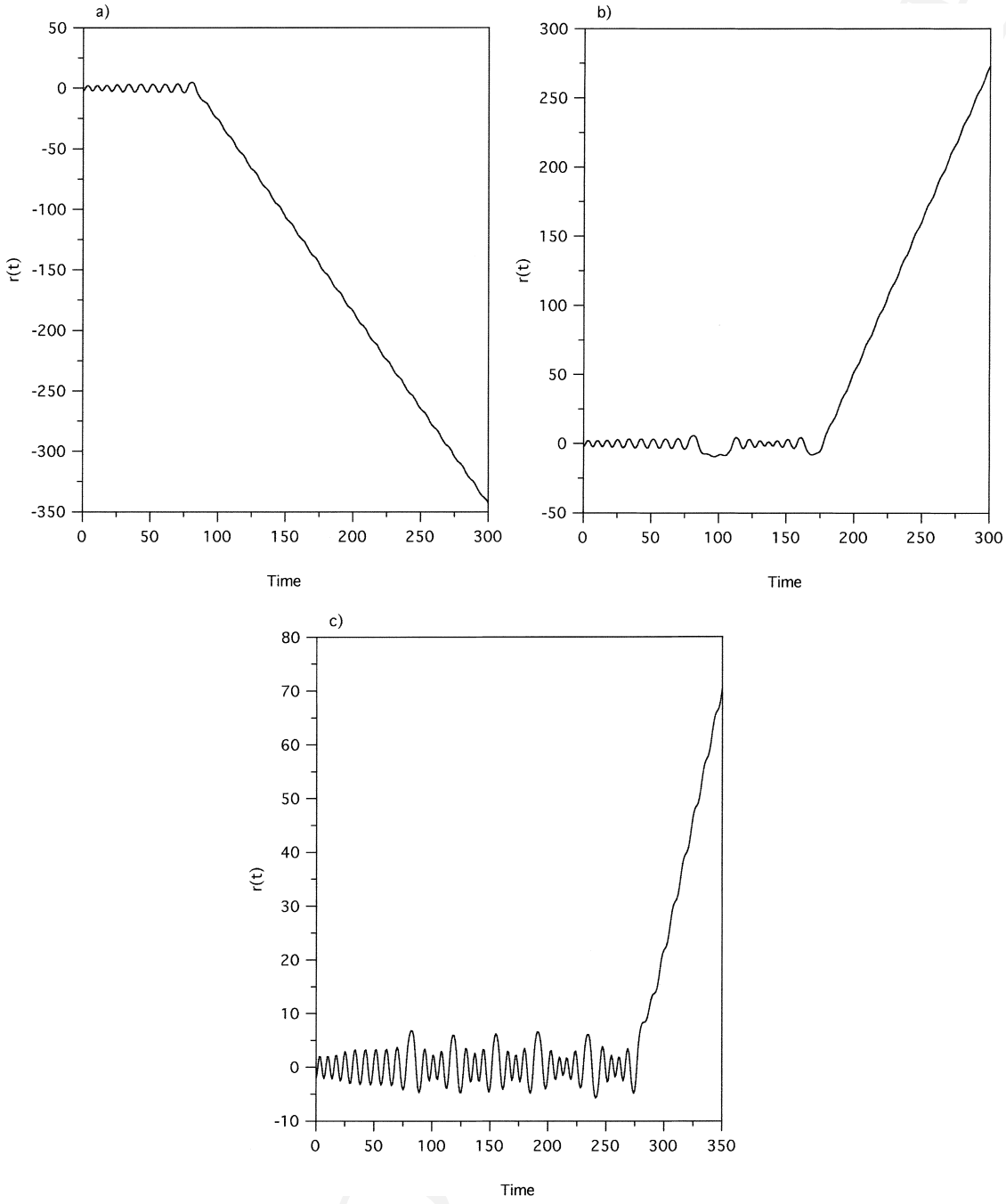

Fig. 6. Plot of $r(t)$ showing breather breakup into K–A pair for the driving frequency 0.7, breather frequency 0.9 and three different amplitudes. (a) Driver amplitude = 0.119765; (b) driver amplitude = 0.119768; (c) driver amplitude = 0.119770. In these cases the driver was turned on gradually over 20 time units starting at $t = 10$.

4. Discussion and conclusions

Previously the authors of [7] investigated the breakup of the SG breather into K and A by a time-independent constant force and obtained good agreement between their theory and their numerical results. In a comprehensive review paper on "Solitons in nearly integrable systems" [8] the authors carried out extensive investigations of several problems including kink–antikink interactions and breather dynamics using general perturbation induced evolution equations for the parameters where the time dependence of the parameters arises solely from the perturbation. They obtained results for a range of problems from breakup of the breather into kink and antikink and for cases with external damping and driving terms, including the results of [7]. The most fundamental difference of our approach from theirs is that the CV, $r(t)$, has time dependence even without a perturbation that gives the rigorous analytic solution, using the Matsuda identity, for the breather solution to the SG partial differential equation. Any external perturbation only produces a change in the time dependence of the solution of the $r(t)$ equation of motion which in turn causes a change in the breather time dependence. Consequently the time-dependent change in the spectra of $r(t)$ due to the perturbation directly, using the Matsuda identity leads to the change of the time-dependent spectra of the SG breather.

The good agreement between S and CV below breakup of the breather into K and A for the parameter range we use in this paper indicates the dominate effect on the breather by the a.c. driver is to change the distance, $r(t)$, between the center of masses of the bound K and A that constitutes the breather from the value of $r(t)$ in the undriven breather. Consequently the change in slope, $\Gamma(t)$, is small or zero in the cases we consider. Note the spatially independent a.c. driver is very different than cases where the breather experiences a spatially dependent driver. In those cases the driver often causes the slope to oscillate. The reason the slope Γ is constant or nearly constant for the a.c. driver (away from breakup) as opposed to the spatially dependent driver is that if you introduce $\Gamma(t)$ as a CV and work out the rigorous equations of motion for $\Gamma(t)$ you find that the a.c. driver does not appear in the Γ equation of motion. The reason is that the breather shape mode is orthogonal to the a.c. driver (see [5]). Thus the only way that $\Gamma(t)$ can develop a time dependence is through the interaction with $r(t)$ which is directly driven by the a.c. driver. For the parameter range we use in this paper the only place where the Γ slope mode could start to oscillate is at the breakup of the breather into K and A where the slope is altered at breakup. Parenthetically the time dependence of the slope in Fig. 1 is not directly due to the a.c. driver but is a consequence of the initial condition at $t = 0$ of the a.c.-driven SG equation.

In [3] the authors expressed their results for the damped a.c.-driven SG in terms of a constant frequency modulation. We can also express our undamped results as a frequency modulation by solving Eq. (2.2) for $\theta(t)$ in terms of $r(t)$ and then taking the time derivative of $\theta(t)$ which is the time-dependent frequency modulation (which depends only on $r(t)$ and $\dot{r}(t)$). In the present paper, we are only considering the undamped case so the frequency modulation is an oscillatory function of time with a rich spectra of frequencies which appear in our wavelet transforms. From the wavelet transform we see that below breakup the frequencies that appear in the phonon band are due to the nonlinearity in the difference between the driven and undriven $r(t)$ caused by the a.c. driver.

The results on the a.c.-driven SG suggest a set of problems worth pursuing. When damping is added to the SG in the underdamped limit there will be a range of phenomena such as those that appear in the treatments of the underdamped pendulum which would apply to the $r(t)$ equation of motion. Then with the use of the Matsuda identity we could find the new breather behavior of the SG that results from the corresponding $r(t)$ behavior. A second area of study would be the effect of moderately stronger drivers even though the agreement would not be as good as the weaker drivers quantitatively but the qualitative agreement would still be good. The case of damped driven SG has been treated in [9–11] and it would be interesting to compare those results with the present approach using CV. A fourth region worth studying further is driving at frequencies in resonance with the breather. Finally the

behavior of $r(t)$ might be an interesting tool for investigating the chaotic nature of the breakup.

References

[1] C.D. Ferguson, C.R. Willis, Physica D 119 (1998) 283.
[2] T. Matsuda, Lett. Nuovo Cimento 24 (1979) 207.
[3] P.S. Lomdahl, M.R. Samuelsen, Phys. Rev. A 34 (1986) 664.
[4] W.H. Press, B.P. Flannery, S.A. Teukolsky, W.T. Vetterling, Numerical Recipes, Cambridge University Press, Cambridge, 1989.
[5] W.C. Lang, K. Forinash, Am. J. Phys. 66 (1998) 794.
[6] R. Boesch, C.R. Willis, Phys. Rev. B 42 (1990) 2290.
[7] P.S. Lomdahl, O.H. Olsen, M.R. Samuelsen, Phys. Rev. A 29 (1984) 350.
[8] Y. Kivshar, B. Malomed, Rev. Mod. Phys. 61 (1989) 763.
[9] J.D. Kaup, A. Newell, Phys. Rev. B 18 (1978) 5162.
[10] R. Grauer, Y. Kivshar, Phys. Rev. E 48 (1993) 4791.
[11] B. Birnir, R. Grauer, Commun. Math. Phys. 162 (1994) 539.